Estimation of Measurement Uncertainty Caused by Surface Gradient for White Light Interferometer

MINGYU LIU, CHI FAI CHEUNG*, MINGJUN REN AND CHING-HSIANG CHENG

Partner State Key Laboratory of Ultra-precision Machining Technology, Department of Industrial and Systems Engineering, The Hong Kong Polytechnic University, Kowloon, Hong Kong
**Corresponding author: benny.cheung@polyu.edu.hk*

Received XX Month XXXX; revised XX Month, XXXX; accepted XX Month XXXX; posted XX Month XXXX (Doc. ID XXXXX); published XX Month XXXX

Although the Scanning White Light Interferometer can provide measurement results with sub-nanometer resolution, the measurement accuracy is far from perfect. The surface roughness and surface gradient have significant influence on the measurement uncertainty since the corresponding height differences within a single CCD pixel cannot be resolved. This paper presents an uncertainty estimation method for estimating the measurement uncertainty due to the surface gradient of the workpiece. The method is developed based on the mathematical expression of an uncertainty estimation model which is derived and verified through a series of experiments. The results show that there is a notable similarity between the predicted uncertainty from the uncertainty estimation model and the experimental measurement uncertainty, which demonstrates the effectiveness of the method. With the establishment of the proposed uncertainty estimation method, the uncertainty associated with the measurement result can be determined conveniently.

OCIS codes: *(120.0120) Instrumentation, measurement, and metrology; (120.3180) Interferometry; (120.3940) Metrology.*

http://dx.doi.org/10.1364/AO.99.099999

1. INTRODUCTION

The Vertical Scanning White Light Interferometer (WLI) has been extensively used as an emerging non-contact optical measurement instrument for ultra-precision surfaces. The accuracy of the measurement result is very high and most of the commercial WLI can provide sub-nanometer resolution [1, 2]. However, the overall uncertainty of the measurement result is usually not given in the instrument’s specifications. Unlike the laser interferometer which uses a stabilized laser as its light source, the WLI makes use of the white light with broad spectrum. As a result, the WLI requires a highly accurate artifact for calibration to reduce the systematic errors. Other calibration processes should be performed to reduce the error caused by the deformation of the sensor and mechanical imperfection [3]. However, even after a very careful calibration process, only the systematic errors can be corrected and the random errors still exists. As early as 1990, Hillmann [4] pointed out that the accuracy of optical measurement is questionable. The measurement result of the optical instrument had significant deviation as compared to a stylus profilometer system.

The environmental issues such as temperature fluctuation and vibration, and the optical noise contribute to the overall measurement uncertainty of the WLI. Previous studies found that the measurement uncertainty is also affected by surface roughness [5, 6] due to the limited resolution of a single pixel of the CCD. The influence was derived theoretically and experimentally with a coherence peak correlogram evaluation method. The influence of the measurement noise was also studied [7–9]. Gao et al. [10] claimed that when measuring surfaces with discontinuity and gradient, the uncertainty of the measurement result can be large. Coupland et at. [11] estimated the measurement error of WLI at space domain using the point spread function. Zhou et al. [12] proposed a random ball test (RBT) method to calibrate the slope-dependent errors in profilometry measurements. It becomes a generally accepted assumption that the measurement uncertainty in the tilt area is significant [13]. In most of the advanced optical components nowadays, the surface discontinuity and gradient become important functional features [14–17]. While measuring these surfaces, the uncertainty of the measurement result varies at different lateral positions due to different surface shape. As a result, it is of practical importance to estimate the uncertainty of the measurement result to verify the conformance of the components since the accuracy requirement is very stringent [18]. Thus far, the quantitative determination of measurement uncertainty caused by surface gradient has received relatively little attention.

In this paper, the relationship between measurement uncertainty and surface roughness, surface gradient and environmental random error was studied. The batwing effect caused by the diffraction [19] and the ridge effect caused by the

multiple scattering [20, 21] is out of the scope of this study and will not be discussed. An uncertainty estimation method is developed which takes into account of the random error, surface roughness and surface gradient is derived in detail using the mathematical method. A series of repeated experiments including measurements for a step height standard, a tilted flat surface, a spherical surface and a diamond-turned freeform surface are conducted to verify the proposed model. The results show that the patterns of the experimental results agree well with the model predicted results which indicate the effectiveness of the uncertainty estimation model. The successful establishment of the uncertainty estimation model provides an important means to predict the uncertainty associated with the measurement result especially for freeform surfaces where gradient varies at different positions.

2. UNCERTAINTY ESTIMATION MODEL

In this section, the uncertainty estimation model for the WLI due to the surface roughness and surface gradient together with the environmental random error is developed. As a 3D profilometer, the measurement result at every position (x, y) can be denoted as $z_m(x, y)$. Due to the limited lateral spatial resolution of the CCD from the white light interferometer, the height differences within one pixel of the CCD cannot be resolved and the measurement result for each $z_m(x, y)$ is determined in a statistical manner. This is the main source of the measurement uncertainty for measuring a rough surface.

Without losing generality, a 2D profile [6] is used for illustration. Within the measurement range of one single pixel of the CCD, the height differences of the workpiece cannot be laterally revolved. The measurement result is affected by the light coming from the specified measurement range. The coherence light also results in the speckle pattern. The effect of the continuum of light illumination is calculated numerically in this study and it is treated as *N* scattering regions, where *N* is a large number. Fig. 1 shows the scattering regions of the flat rough surface. Where the dark solid line denotes the measured surface, $z_j (j = 1, 2, ..., N)$ is the distance from the CCD plane P_o to the jth scattering region, z_o is the surface mean height and $z_o = \frac{1}{N}\sum_{j=1}^{N} z_j$.

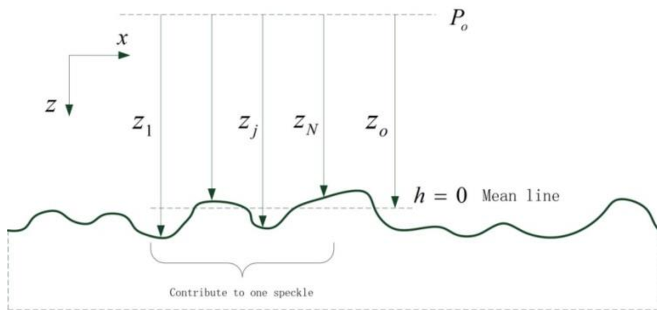

Fig. 1. Flat rough surface [6]

The measurement uncertainty of a flat rough surface can be determined by Eq. (1) [6].

$$\delta_z = \frac{1}{\sqrt{2}}\sqrt{\frac{\langle I \rangle}{I}}\sigma_h \quad \textbf{(1)}$$

where $\langle I \rangle$ is the mean intensity of the speckle pattern, I is the intensity of the individual speckle and σ_h is the standard deviation of the height distribution of the rough surface, under the assumption that $\sigma_h < \frac{1}{4} l_c$, where l_c is the coherence length. σ_h can be determined by Eq. (2).

$$\sigma_h = \sqrt{\frac{1}{N-1}\sum_{j=1}^{N}(z_j - z_o)^2} \quad \textbf{(2)}$$

While considering the surface gradient, it is supposed that the surface is tilted for a certain angle θ as is shown in Fig. 2, where $z_j' = z_j - j\Delta h$, Δh is the average height difference for a nearby scattering region and it can be determined by $\Delta h = \frac{d}{N}\tan\theta$, where d is the dimension of a single pixel of the CCD.

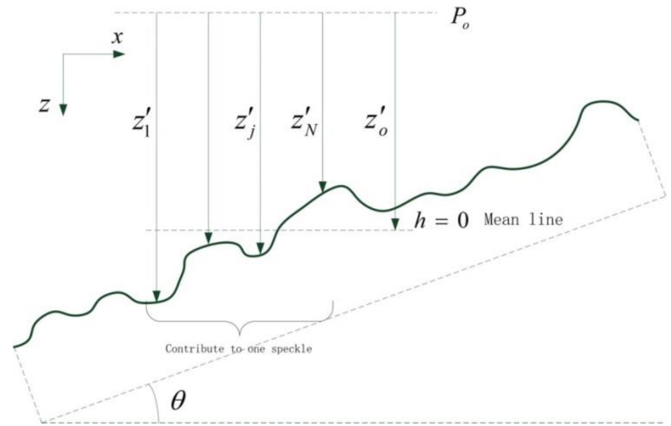

Fig. 2. Tilted rough surface

When N is very large, the mean of the tilted surface z_o' can be determined by

$$\begin{aligned} z_o' &= \frac{1}{N}\sum_{j=1}^{N} z_j' = \frac{1}{N}\sum_{j=1}^{N}\left(z_j - j\Delta h\right) \\ &= z_o - \frac{(N+1)\Delta h}{2} = z_o - \frac{1}{2} d\tan\theta \end{aligned} \quad \textbf{(3)}$$

Hence, the standard deviation of the height of the tilted surface can be derived and determined by Eq. (4).

$$\begin{aligned} \sigma_h'^2 &= \frac{1}{N-1}\sum_{j=1}^{N}\left(z_j' - z_0'\right)^2 \\ &= \frac{1}{N-1}\sum_{j=1}^{N}\left[\left(z_j - j\Delta h\right) - \left(z_o - \frac{(N+1)\Delta h}{2}\right)\right]^2 \\ &= \frac{1}{N-1}\sum_{j=1}^{N}\left[\left(z_j - z_o\right) - \left(j\Delta h - \frac{(N+1)\Delta h}{2}\right)\right]^2 \\ &= \frac{1}{N-1}\sum_{j=1}^{N}\left[\left(z_j - z_o\right)^2 + \left(j - \frac{(N+1)}{2}\right)^2 \Delta h^2 \right. \\ &\qquad \left. - 2\Delta h\left(z_j - z_o\right)\left(j - \frac{(N+1)}{2}\right)\right] \\ &= \sigma_h^2 + \frac{1}{N-1}\left[g\Delta h^2 - 2\Delta h f(z_1, z_2, ..., z_N)\right] \end{aligned} \quad \textbf{(4)}$$

where $f(z_1, z_2, ..., z_N)$ is determined by

$$f(z_1, z_2, ..., z_N) = \sum_{j=1}^{N} \left[\left(z_j - z_o \right) \left(j - \frac{(N+1)}{2} \right) \right] \quad \textbf{(5)}$$

and g is determined by

$$\begin{aligned} g &= \sum_{j=1}^{N} \left(j - \frac{(N+1)}{2} \right)^2 \\ &= \sum_{j=1}^{N} N^2 + N(N+1)^2/4 - (N+1)(N+1)N/2 \\ &= N(N+1)(N-1)/12 \end{aligned} \quad \textbf{(6)}$$

Since σ_h is the statistical result of $(z_j - z_o)(j = 1, 2, \cdots, N)$ which is determined by Eq. (2) and

$$\sum_{j=1}^{N} \left[j - \frac{(N+1)}{2} \right] = (1 + 2 + ... + N) - N(N+1)/2 = 0 \quad \textbf{(7)}$$

So, statically, $f(z_1, z_2, ..., z_N) \approx 0$. Hence,

$$\sigma_h'^2 = \sigma_h^2 + \frac{1}{12} d^2 \tan^2 \theta \quad \textbf{(8)}$$

Practically, $d \tan \theta$ can be calculated by the numerical gradient in x direction. Hence, for a 3D surface $z_m(x, y)$, σ_h' can be determined by

$$\sigma_h'^2 = \sigma_h^2 + \frac{1}{12} \left[\left(\frac{\partial z_m}{\partial x} \Delta x \right)^2 + \left(\frac{\partial z_m}{\partial y} \Delta y \right)^2 \right] \quad \textbf{(9)}$$

where Δx and Δy are the lateral dimensions of the single pixel of the CCD along x and y directions, respectively.

Thus, the measurement uncertainty of the tilted rough surface can be determined by

$$\delta_t' = \sqrt{\frac{1}{2} \frac{\langle I \rangle}{I} \left(\sigma_h^2 + \frac{1}{12} \left[\left(\frac{\partial z_m}{\partial x} \Delta x \right)^2 + \left(\frac{\partial z_m}{\partial y} \Delta y \right)^2 \right] \right)} \quad \textbf{(10)}$$

With the use of the uncertainty propagation method [20], the total uncertainty contributed from surface roughness and surface gradient together with environmental random error can be determined by Eq. (11)

$$\delta_t' = \sqrt{\frac{1}{2} \frac{\langle I \rangle}{I} \left(\sigma_h^2 + \frac{1}{12} \left[\left(\frac{\partial z_m}{\partial x} \Delta x \right)^2 + \left(\frac{\partial z_m}{\partial y} \Delta y \right)^2 \right] \right) + \delta_r^2} \quad \textbf{(11)}$$

where δ_r is the random error introduced by the environmental issue.

It is interesting to note from Eq. (11) that the overall measurement uncertainty is affected by the surface roughness, the surface gradient and the lateral resolution (which is determined by the object lens and the size of a single CCD pixel) and the environmental random error. With a carefully controlled environment with little vibration and temperature fluctuation, the environmental random error is insignificant. Another factor is that the size of the single CCD pixel is inherently fixed. As a result, most of the uncertainty is caused by the surface roughness and gradient together with the object lens used. With a surface of larger roughness, larger local gradient and a lower magnification object lens, the measurement uncertainty is larger, and vice versa. According to the proposed model, once the measurement result is obtained, the uncertainty associated with the measurement result can be estimated. Fig. 3 shows the measurement uncertainty map under different surface roughness, gradient and object lens.

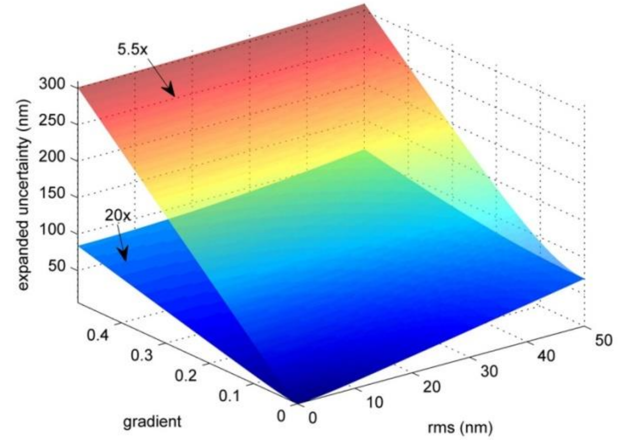

Fig. 3. Uncertainty map for different roughness, gradient and object lens

3. EXPERIMENT VERIFICATION AND DISCUSSION

To evaluate the estimation performance of the proposed uncertainty estimation model, the type A evaluation of standard uncertainty [22] was used to determine the measurement uncertainty. In this study, the expanded uncertainty is used instead of standard uncertainty in order to obtain a better coverage factor. According to the Central Limit Theorem [23], the measurements should be governed by normal distribution. A series of repeated experiments were performed using a commercial white light interferometer - Zygo® Nexview™. Measurements of the standard height artifact were firstly performed. The heights were then determined with the measurement results and the standard deviations of the height values were determined. This was used to calculate the uncertainty caused by environmental noise. A diamond-tuned tilted surface with 4° tilting angle was then measured in order to directly verify the proposed model influenced by surface tilt. Next, measurements of a sphere artifact were performed to verify the proposed model. At last, a diamond-tuned workpiece with micro-lens array was measured to demonstrate the utility of the model for complex surfaces. For the tilted flat surfaces, spherical surface and the complex surface, the measured uncertainties were compared with the estimated uncertainties as derived by the proposed model for verification.

1. Measurement of step height standard

A VLSI step height standard traceable to SI units was used in the experiment. The specification of the step height standard artifact is shown in Table 1, with the environment condition of 21±1°C temperature and 49±2% humidity.

Table 1. Specification of Step Height Standard

Mean Value	1.798 **μm**
Expanded Uncertainty	0.011 **μm**

The step height standard was measured 50 times using two object lenses with different magnifications. Fig. 4 shows one of the measurement results of the step height standard. It should be noted that although it was carefully adjusted to remove the tilting in the measuring process, there was still some residual tilting error. As a result, the height value cannot be calculated by directly subtracting the value from plane A to plane B. In this study, the step height value was calculated using the method below: (i). a plane was fitted as the reference plane (P_{ref}) using data points from plane B. (ii). data points (D_i) from plane A were selected and the distances from D_i to P_{ref} were calculated and the average value was determined to be the measurement result of the step height. Since the step height artifact has an extremely smooth surface, the influence of surface roughness can be ignored.

The same method was applied when measured with the 5.5× and 20× object lens. Fig. 5(a) and Fig. 5(b) show the measurement results in histograms. Normal distributions were also fitted for the data. The mean values and the expanded standard deviations were summarized and shown in Table 2. The result shows that the two measurements are in good agreement with the specification, which indicates that the instrument was well calibrated. The environmental affected random noise can be determined by the expanded standard deviations of the measurements, which are 0.0035µm and 0.0026µm, respectively. From this result, it can be concluded that the environmental random error is only several nanometer, which is negligibly small for most applications.

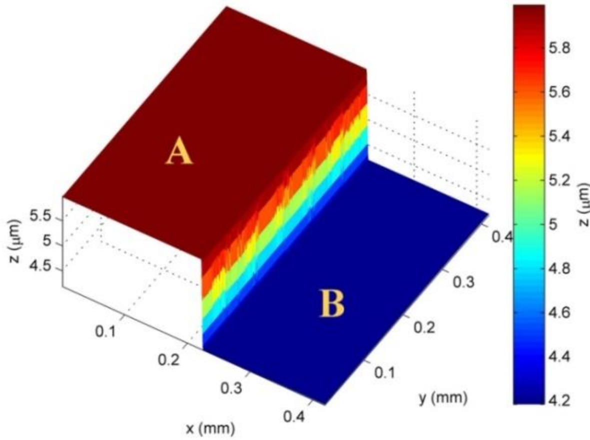

Fig. 4. Measurement result of the step height standard

2. Measurement of diamond-turned titled flat surfaces

A diamond-turned tilted flat surface with tilting angle of 4° was machined to verify the proposed uncertainty estimation model. The surface is shown in Fig. 6(a). Ten times repeated measurements were performed to obtain the measurement uncertainty. The surface was measured with a 20× object lens. It should be noted that in a series of repeated measurements, the results are shifted in z axis which indicates that there is a systematic error in the absolute value of the measurement results. This drift phenomenon was also reported by Zhou et. al. [24] and it exists in all instruments. Fig. 7 shows the results of one pixel in a series of 100 times repeated measurements. In this experiment, the aggregated z axis shift is about 1µm and it is in a decreasing

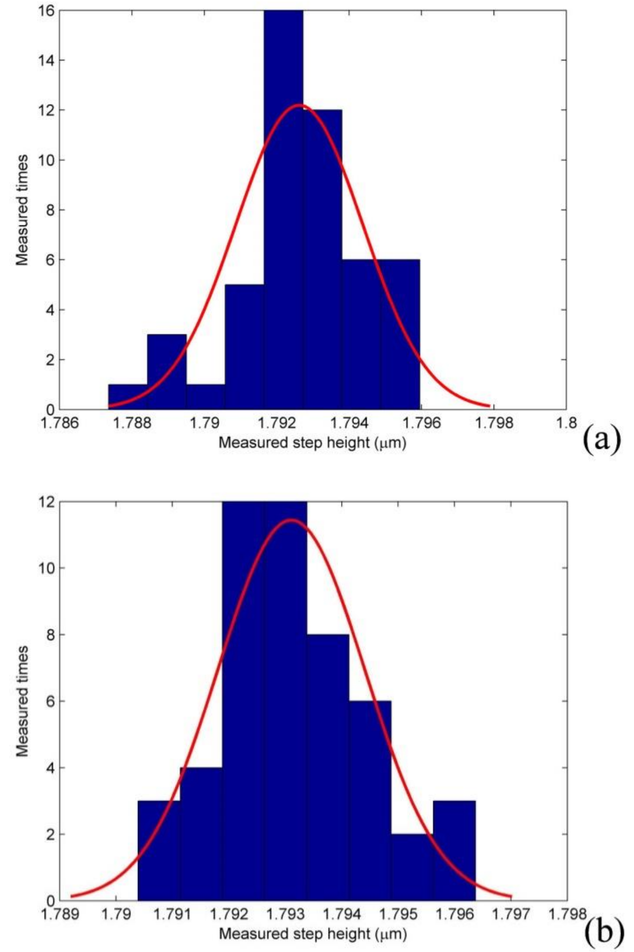

Fig. 5. Histograms with fitted normal distributions. (a) 5.5× object lens. (b) 20× object lens

Table 2. Mean and expanded uncertainty of the step height Measurements

Object lens	5.5×	20×
Mean Value	1.7926 **μm**	1.7932 **μm**
Expanded Uncertainty	0.0035 **μm**	0.0026 **μm**

manner. The shifting value is significant as compared with the measurement uncertainty. As a result, preprocessing for the measurement data is needed to eliminate the z axis shift. First, the relatively flat area was chosen to calculate the surface mean height since the flat surface has a smaller measurement uncertainty. Second, the mean height was subtracted from the original measurement result to generate the data without z axis shifting.

After removing the z axis shift, the measurement uncertainty was calculated for each pixel position (x, y) and the result is shown in Fig. 6(b). The estimated uncertainty using the developed model was also calculated with the conditions where $\langle I \rangle / I = 1$, $\sigma_h = 2nm$ and $\delta_r = 0.0026\mu m$, and the result is shown in Fig. 6(c). The result shows that the measurement uncertainty is low in the flat area, which is expected. In contrast, the measurement uncertainty in the titled flat surface is high. There is a step change

in terms of the surface gradient and this can be reflected in both measurement and estimation results.

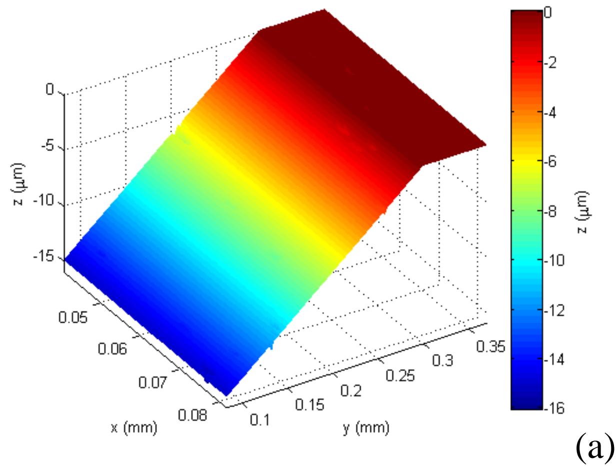

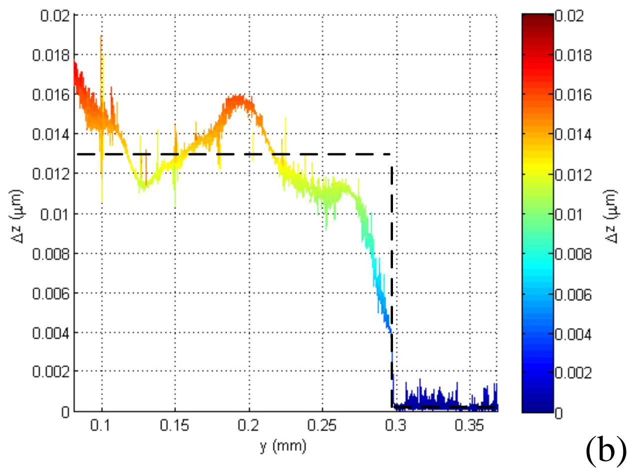

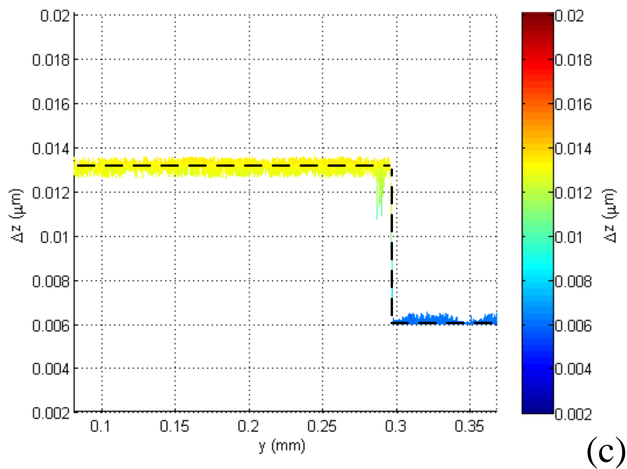

Fig. 6. 4° tilted flat surface, measured with 20× object lens. (a) Measurement result. (b) Experimental uncertainty. (c) Estimated uncertainty

In this experiment, it is interesting to note that there were machining defects in the surface where the local gradient were large and caused much noise in the experimental uncertainty and estimated uncertainty. In order to better illustrate the performance of the model, the noise in both results was removed. The dash line in Fig. 6(b) and Fig. 6(c) denotes the mean value of the experimental uncertainty and estimated uncertainty, respectively. The upper bound values match very well with the value about 13nm. It is found that there is fluctuation in the experimental uncertainty. This fluctuation may be caused by the ratio deviation of $\langle I \rangle / I$, which is assumed to be 1 in the model.

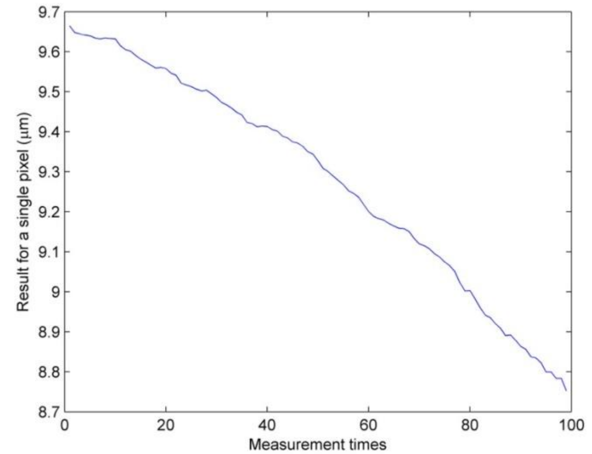

Fig. 7. z axis shift for repeated measurements.

3. Measurement of spherical surface

A spherical artifact calibrated by NAMAS (National Measurement Accreditation Service) with a diameter of 21.9874mm was chosen for the verification with the benefit that the artifact has different surface gradients at different lateral positions and its surface is very smooth. Fig. 8 shows the measurement result of the surface, the uncertainty calculated from repeated experiments, the estimated uncertainty and the estimation errors. The estimated uncertainty using the developed model is calculated with the conditions where $\langle I \rangle / I = 1$, $\sigma_h = 1nm$ and $\delta_r = 0.0026\mu m$. The central part of the surface is relatively flat while the outer part of the surface has a larger surface gradient. The experimental result and the estimation result are found to be in good agreement with the result that the uncertainty in the central part is relatively low while the uncertainty in the outer part is relatively large. The result of estimation error is shown in Fig. 8(d). It shows that the error of most of the estimation results within the central part is less than 5nm and the outer part is larger with an estimation error of about 10nm. In the experimental result, it is very interesting to find that, the uncertainty is slightly distributed as an elliptical shape while the estimation result appears to possess a circular shape. The ellipse-shape uncertainty distribution phenomenon may come from the inherent unbiased alignment of the measurement equipment, which is needed for further study.

Three measurement points with different local gradients on the sphere surface which marked as “1”, “2” and “3” were analyzed and the result is shown in Fig. 9. The data marked with circle is the experimental uncertainty while the data marked with star denotes the estimated uncertainty. The result shows that when the surface gradient increases (gradient: 1 < 2 < 3), the experimental uncertainty and the estimated uncertainty increase in a similar manner. The prediction error is about several nanometer which indicates the effectiveness of the proposed model.

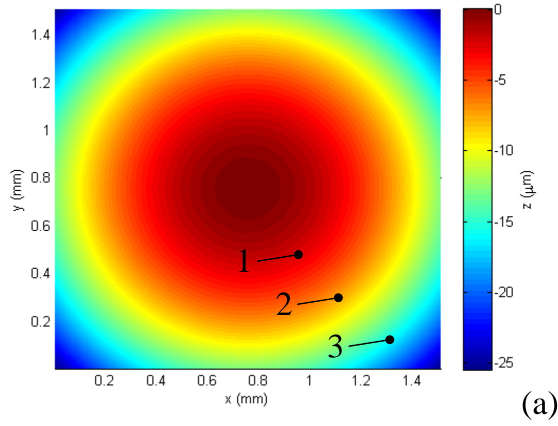

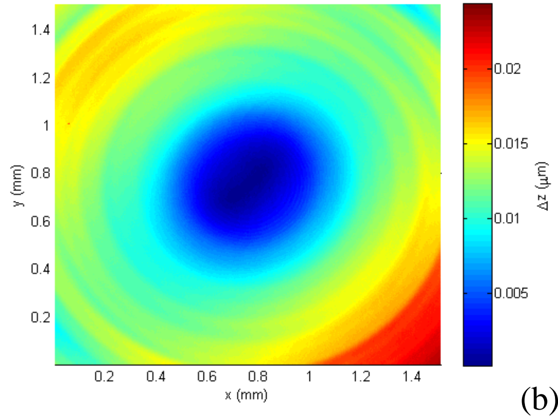

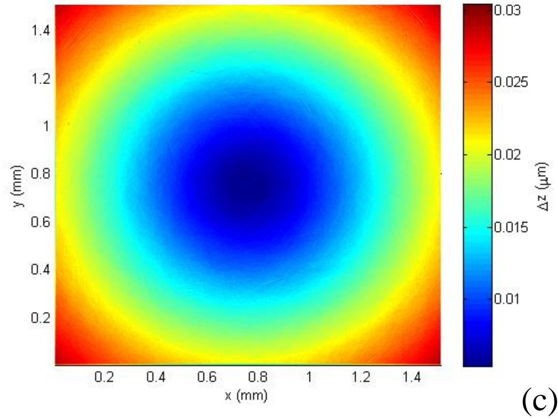

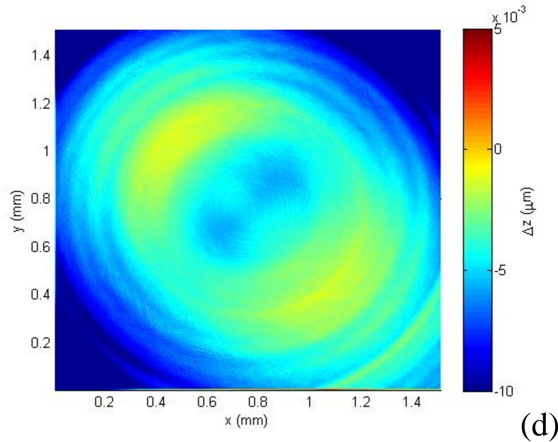

Fig. 8. Spherical surface, measured with 5.5× object lens. (a) Measurement result. (b) Experimental uncertainty. (c) Estimated uncertainty. (d) Estimation error

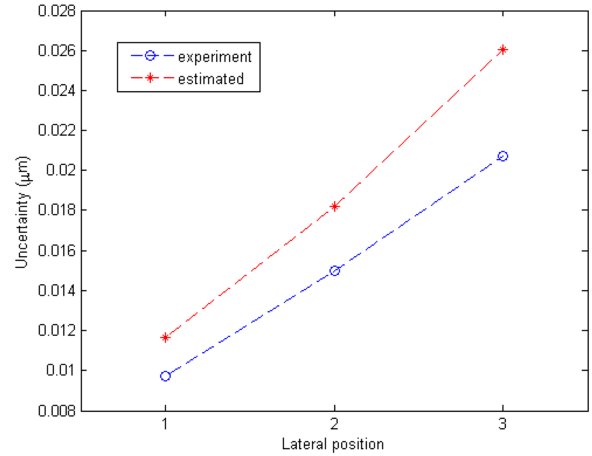

Fig. 9. Experimental uncertainty and estimated uncertainty in 3 position with different gradients.

4. Measurement of complex surfaces

A diamond-turned micro-lens array was chosen to demonstrate the measurement of complex freeform surfaces. For this workpiece, 50 times repeated measurements were performed. The micro-lens array surface was then measured with a 5.5× object lens. Similarly to the previous subsection, since the result is shifted in the repeated measurement, preprocessing of the measurement data is needed. The estimated uncertainty using the developed model is calculated with the conditions where $\langle I \rangle / I = 1$, $\sigma_h = 5nm$ and $\delta_r = 0.0035\mu m$. The result is shown in Fig. 10 which shows that the patterns have very high similarity. In general, the uncertainty in the relatively flat area is small while the uncertainty in the area of the edge within the micro-lens array is large, which is correctly estimated in the model and verified in the experiment. Even in the area with tool marks and defects, where the measurement uncertainty is large due to the local gradient, the uncertainty can also be correctly estimated and can be matched with the results of the repeated measurement.

Though the patterns have high similarity and the uncertainties are consistent with the proposed model, there are still uncertainties between the model and reality. The predicted uncertainty value may have certain deviation from the experimental value. This may be caused by the following reasons: (i) The difference may come from the data processing method. In this research, the multiple measurement results are aligned using the relative flat surface as reference. The calculated uncertainty in those areas may be under estimated. This may also affect the result for other areas. Nevertheless, the impact of this issue is relatively small. As a result, the overall trend of the estimation can match the experimental value closely. (ii) In the estimation model, the value of $\langle I \rangle / I$ is unknown and it was chosen to be 1 in the calculation. This is another source of the prediction uncertainty.

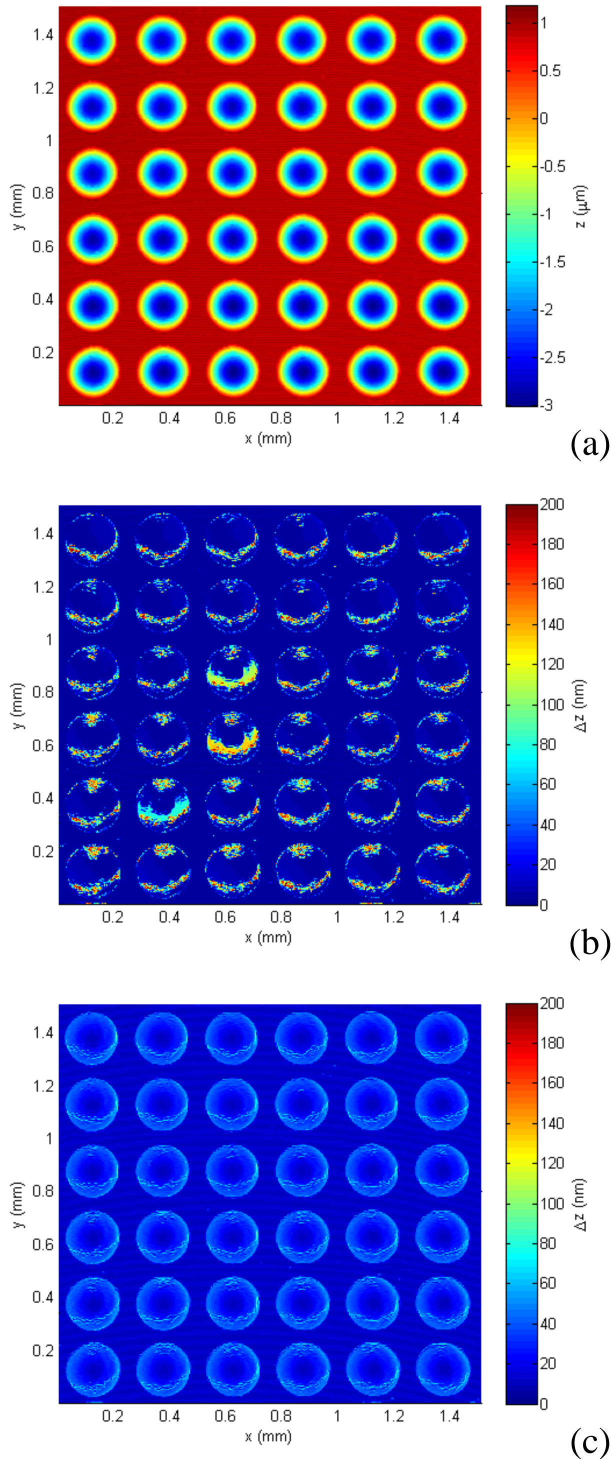

Fig. 10. Micro-lens array with 5.5× object lens. (a) Measurement result. (b) Experimental uncertainty. (c) Estimated uncertainty

4. CONCLUSION

The Scanning White Light Interferometer is frequently used for precision measurement since it is a non-contact optical metrology instrument that can provide sub-nanometer resolution result. However, the uncertainty of measurement results for some kinds of surfaces can be large which is caused by roughness and local gradient. This study established an estimation model and hence a method to predict the measurement uncertainty for these surfaces and a series of experiments were conducted to verify the effectiveness of the proposed model. The results show that the uncertainty predicted from the model and the experiments have good agreement.

It can be concluded that the overall measurement uncertainty is affected by the surface roughness and gradient, whose mathematical expression as derived in Eq. (11). The uncertainty is large at the area where local surface gradient is large and measured with a low magnification object lens, and vice versa. With the establishment of the uncertainty estimation model, the uncertainty associated with the measurement result can be predicted well. In the applications where accuracy requirement is stringent and large local gradient exists, much attention should be paid. Since the measurement error is of Gaussian distribution, it is suggested to perform multiple measurements and fit a Gaussian curve to the measurement results to find the best estimated value for each lateral position.

Even the estimation results have good agreement with the experimental results, the model is developed on some assumptions and approximations, e.g. $\langle I\rangle/I$ is assumed to be constant. Some special cases such as the batwing and ridge effects are not discussed. The estimation performance may have significant deviation due to the above reasons. Further investigations will be conducted to improve the performance of the proposed model to overcome the limitation.

Funding. PhD studentship from The Hong Kong Polytechnic University (RTHC).

Acknowledgment. The work was supported by a PhD studentship from The Hong Kong Polytechnic University (project account code: RTHC). The authors would also like to express their sincerely thank to the technical staff from Partner State Key Laboratory of Ultra-precision Machining Technology in the Department of Industrial and Systems Engineering at The Hong Kong Polytechnic University for their technical support to this research work.

References

1. Zygo Corporation. Nexview 3d optical surface profiler. 2015.
2. Veeco Instruments Inc. Wyko nt series optical profilers. 2009.
3. Leach R. Optical measurement of surface topography: Springer, 2011.
4. Hillmann W, Kunzmann H. Surface profiles obtained by means of optical methods—are they true representations of the real surface? CIRP Annals-Manufacturing Technology. 1990;39:581-3.
5. Pavliček P, Hýbl O. White-light interferometry on rough surfaces--measurement uncertainty caused by surface roughness. Applied optics. 2008;47:2941-9.
6. Pavliček P, Soubusta J. Theoretical measurement uncertainty of white-light interferometry on rough surfaces. Applied optics. 2003;42:1809-13.
7. Pavliček P, Hýbl O. White-light interferometry on rough surfaces—measurement uncertainty caused by noise. Applied optics. 2012;51:465-73.
8. Pavliček P, Michálek V. White-light interferometry—envelope detection by Hilbert transform and influence of noise. Optics and Lasers in Engineering. 2012;50:1063-8.
9. Hering M, Körner K, Jähne B. Correlated speckle noise in white-light interferometry: theoretical analysis of measurement uncertainty. Applied optics. 2009;48:525-38.
10. Gao F, Leach RK, Petzing J, Coupland JM. Surface measurement errors using commercial scanning white light interferometers. Measurement Science and Technology. 2008;19:015303.
11. J. Coupland, R. Mandal, K. Palodhi, and R. Leach, "Coherence scanning interferometry: linear theory of surface measurement," Applied optics 52, 3662-3670 (2013).

12. Y. Zhou, Y.-S. Ghim, A. Fard, and A. Davies, "Application of the random ball test for calibrating slope-dependent errors in profilometry measurements," Applied optics 52, 5925-5931 (2013).
13. Henning A, Giusca C, Forbes A, Smith I, Leach R, Coupland J, et al. Correction for lateral distortion in coherence scanning interferometry. CIRP Annals - Manufacturing Technology. 2013;62:547-50.
14. Kim GD, Loh BG. An ultrasonic elliptical vibration cutting device for micro V-groove machining: Kinematical analysis and micro V-groove machining characteristics. Journal of Materials Processing Technology. 2007;190:181-8.
15. Yabu H, Shimomura M. Simple fabrication of micro lens arrays. Langmuir. 2005;21:1709-11.
16. Yan JW, Maekawa K, Tamaki J, Kuriyagawa T. Micro grooving on single-crystal germanium for infrared Fresnel lenses. Journal of Micromechanics and Microengineering. 2005;15:1925-31.
17. Xie J, Zhuo YW, Tan TW. Experimental study on fabrication and evaluation of micro pyramid-structured silicon surface using a V-tip of diamond grinding wheel. Precis Eng. 2011;35:173-82.
18. Jiang X. In situ real-time measurement for micro-structured surfaces. CIRP Annals-Manufacturing Technology. 2011;60:563-6.
19. Harasaki A, Wyant JC. Fringe modulation skewing effect in white-light vertical scanning interferometry. Applied Optics. 2000;39:2101-6.
20. Coupland J, Lobera J. Measurement of steep surfaces using white light interferometry. Strain. 2010;46:69-78.
21. Gao F, Coupland J, Petzing J. V-groove measurements using white light interferometry. Photon06, Manchester. 2006:4-7.
22. BIPM, IEC, IFCC, ISO, IUPAC, OIML. Guide to the Expression of Uncertainty in Measurement. International Organisation for Standardization, Geneva, Switzerland. 1993.
23. Taylor JR. An Introduction To Error Analysis: The Study Of Uncertainties In Physical Measurements Author: John R. Taylor, Publisher. 1996.
24. Zhou Y, Fard AP, Davies A. Characterization of instrument drift using a spherical artifact. Precision Engineering. 2014;38:443-7.